Available online at www.sciencedirect.com

ScienceDirect

Energy Procedia 151 (2018) 69–73

Energy Procedia

www.elsevier.com/locate/procedia

3rd Annual Conference in Energy Storage and Its Applications, 3rd CDT-ESA-AC, 11–12 September 2018, Sheffield, UK

CuHCF as an electrode material in an aqueous dual-ion Al^{3+}/K^{+} ion battery

Alexander Holland[a]*, Harriet Kimpton[a], Andrew Cruden[a], Richard Wills[a]

[a] *University of Southampton, University Road, Southampton, SO17 1BJ*

Abstract

Copper-hexacyanoferrate (CuHCF) is capable of 28000 cycles in 1 mol dm^{-3} $AlCl_3$ in a 3-electrode cell, while performance improves with the addition of K^+. However, CuHCF synthesised by co-precipitation is in a partially oxidised state, resulting in an effective state-of-charge (SoC) of 90%. Chemical reduction is possible by soaking electrodes in 10 mmol dm^{-3} $Na_2S_2O_3$ to produce an electrode at 0% SoC, while chemical oxidation in 100 mmol dm^{-3} $KMnO_4$ is possible in order to produce electrodes at 100% SoC. Despite this, a full cell constisting of a TiO_2 negative electrode, CuHCF positive electrode and 1 mol dm^{-3} $AlCl_3$/1 mol dm^{-3} KCl, allows ca. 1100 cycles due to the premature degradation of CuHCF. This is due to the low coulombic efficiency (CE) of TiO_2, which results in consistent overcharging of CuHCF and the likely loss of Fe^{3+} to the electrolyte.

Selection and peer-review under responsibility of the 3rd Annual Conference in Energy Storage and Its Applications, 3rd CDT-ESA-AC.

Keywords: Hybrid aluminium-ion, TiO_2, CuHCF, aqueous battery, high-rate

1. Introduction

Li-ion batteries have become ubiquitous in portable electronics, look set to deliver the first wave of electric cars and are also widely being used within power grids to maintain reliability. However, a number of alternative technologies are being researched to provide improvements to metrics such as cost, safety, environmental impact, power capability and energy density [1-3]. Aqueous intercalation batteries could improve upon the safety, environmental impact and power of current Li-ion chemistries [4]. Specifically, prussian blue analogues such as copper-hexacyanoferrate (CuHCF), are capable of up to 40 000 cycles at specific currents of the order of A g^{-1} in a

* Corresponding author. Tel.: +44773784034
E-mail address: awh1g10@soton.ac.uk

Selection and peer-review under responsibility of the 3rd Annual Conference in Energy Storage and Its Applications, 3rd CDT-ESA-AC.
10.1016/j.egypro.2018.09.029

variety of aqueous electrolytes [5]. While capacity of the electrode is relatively low at ca. 40-50 mA h g^{-1}, specific energy is likely to be greater than supercapacitors (<20 mW h g^{-1}) - a reasonable comparison given its high cycle life and rate capability. With a suitable negative electrode, CuHCF could be desirable for applications such as power smoothing or regenerative breaking. However outside of aqueous Li-ion, there is a relative dearth of negative electrodes suitable for pairing into a full aqueous intercalation cell [6, 7]. As such, full aqueous-ion cells have used activated carbon as the negative electrode, with its limited capacity and unfavorable voltage profile [8, 9].

Here, CuHCF is coupled with anatase-TiO_2, which has shown promising performance in aqueous Al^{3+} electrolyte, itself a desirable working ion due to the high abundance of aluminium. First, both chemical oxidation and reduction of CuHCF are shown to be possible, enabling construction of a full cell with both negative and positive electrodes in their desried SoC. Second, CuHCF is shown to have a considerably greater cycle life in $AlCl_3$ than previously reported, likely due to the more rigorous electrode manufacture procedure used. Finally, the performance and degradation of CuHCF in a full cell using anatase-TiO_2 as the negative electrode is explored.

2. Experimental procedures

CuHCF was synthesised via a co-precipitation method previously reported [5]. Electrodes were manufactured through shear mixing of CuHCF or TiO_2, carbon black (10 wt% for CuHCF and 5 wt% for TiO_2) Nafion binder (7.5 wt%) and propanol at 5000 rpm for 30 minutes using a Silverson shear mixer. Inks were coated onto carbon polymer current collectors from Sigracell and allowed to dry in ambient conditions.

The full cell consisted of TiO_2 and CuHCF in a 1.5:1 mass ratio and 1 mol dm^{-3} $AlCl_3$/1 mol dm^{-3} KCl electrolyte. 3-electrode cells used oversized CuHCF electrodes as counter and a saturated calomel reference electrode (SCE). Electrochemical measurements were performed on a Solartron battery analyser. UV-vis spectroscopy was performed on a Varian Cary 300 Bio spectrophotometer over a wavelength of 200 to 900 nm with base-fluid correction (water) being undertaken using the same base-fluid and a 10 mm (path length) quartz cuvette. Ex-situ XRD was performed on a Rigaku MiniFlex 600.

3. Results and discussion

3.1. Tailoring CuHCF state-of-charge

CuHCF synthesised by co-precipitation gives rise to an electrode in a partially charged state. Fig. 1a shows as-synthesised CuHCF to have an initial potential of 0.79 V vs SCE with a corresponding 1st cycle charge capacity of only 4 mA h g^{-1} before reaching 1.0 V vs SCE. The 1st cycle discharge capacity is 35 mA h g^{-1}. It is important to tailor initial state-of-charge (SoC) to match that of the corresponding negative electrode in order to minimize side reactions and allow the capacity of both electrodes to be utilised. Using TiO_2 as the negative electrode, a positive electrode is required to be in a reduced and intercalated state to match the oxidised state of TiO_2. In order to achieve this, CuHCF electrodes were chemically reduced by soaking in a 20 ml solution of 10 Mm $Na_2S_2O_3$ before washing and soaking in de-ionised water and being dried in ambient conditions. In active electrolyte of 1 mol dm^{-3} $AlCl_3$/1 mol dm^{-3} KCl, the open circuit potential (OCP) of CuHCF decreased from 0.79 V to 0.65 V vs SCE after 30 minutes 10 mmol dm^{-3} $Na_2S_2O_3$. This corresponded to a fully reduced and discharged electrode. Soaking times lower than 30 minutes resulted in intermediate OCPs and SoC, while higher concentrations of $Na_2S_2O_3$ resulted in faster reduction of OCP and SoC. Fig. 1b shows the chemically reduced CuHCF to have a 1st cycle capacity of 39.6 mA h g^{-1} with 99.5% coulombic efficiency (CE). Conversely, chemical oxidation in $KMnO_4$ is also possible and was able to increase SoC to 100%, as seen by the initial potential of 0.85 V and intial discharge capacity of 42 mA h g^{-1} seen in Fig. 1c. Neither treatment adversely affected cycle life. Chemical oxidation could be applicable to aqueous, rechargeable Zn-ion batteries as Zn metal will be in a fully charged state, which undergoes dissolution upon the 1st discharge, allowing Zn^{2+} cations to migrate and insert into the positive electrode.

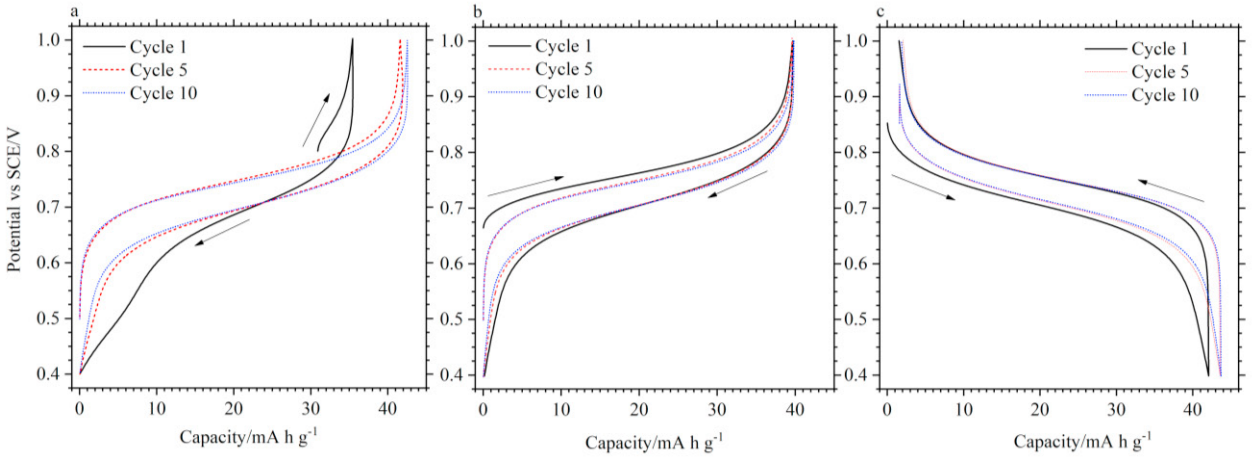

Fig. 1. Voltage profiles of as-synthesised CuHCF (a), chemically reduced CuHCF electrode (b) and oxidized CuHCF (c) vs an SCE reference. Electrolyte was 1 mol dm^{-3} $AlCl_3$/1 mol dm^{-3} KCl and cycling was performed at 1 A g^{-1}.

3.2. Full-cell vs 3-electrode cell

As previously shown, a full aqueous Al-ion cell could be constructed using CuHCF, TiO_2 and $AlCl_3$ [10]. However, while Al^{3+} can be reversibly inserted into CuHCF, performance improved with the addition of K^+, resulting in a dual-ion cell with preferential insertion of K^+ into CuHCF and Al^{3+} into TiO_2. However, the <100% CE of TiO_2 would cause overcharging (under-discharging) of CuHCF compared to TiO_2. Fig. 2a gives the voltage profile of TiO_2 cycled at 0.2, 0.5 and 2.0 A g^{-1} between -1.0 V to +0.4 V vs SCE in a 3-electrode cell. A maximum discharge capacity of 19.1 mA h g^{-1} is seen at 0.2 A g^{-1}. However, CE increases from 88.0% at 0.2 A g^{-1} to 98.8% at 2.0 A g^{-1}, where discharge capacity is 13.9 mA h g^{-1}. The result of this <100% CE is the overcharging of CuHCF and can be observed by examining Fig. 2b, which shows the cycling of a full cell to 30 mA h g^{-1}_{CuHCF} at 1.5 A g^{-1}_{CuHCF}.

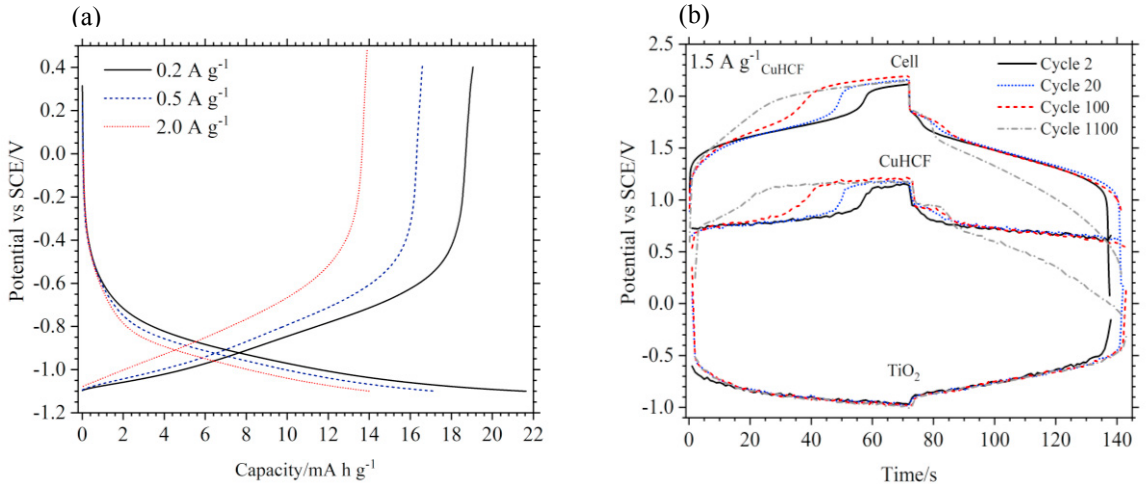

Fig. 2. (a) Voltage profiles of TiO_2 cycled in a 3-electrode cell between -1.1 V - +0.4 V vs SCE at 0.2, 0.5 and 2.0 A g^{-1}. (b) Profiles of CuHCF (positive) and TiO_2 (negative) in a full cell cycled at various C-rates. Cycles shown are of those performed at a 50C C-rate which corresponds to 1.5 A g^{-1}_{CuHCF}. TiO_2 and CuHCF potentials are given vs SCE.

A linear discharge slope occurs at 0.7 V with the onset of a 2nd discharge shoulder arising around 0.9 V during subsequent cycling, in contrast to the flat S-shaped curves in Fig. 1. The onset of the 2nd charge plateau occurs at

earlier stages of the charge phase with subsequent cycles. By the 100th cycle, the onset of the 2nd plateau occurs after approximately 40s and by the 1100th cycle the voltage profile of CuHCF had degraded severely, immediately increasing from 0.6 V to a plateau around 1.1V during the charge phase and sloping down to -0.2 V during discharge. Beyond cycle 1100, CuHCF capacity begins to drop from the initial 30 mA h g^{-1}. The decreasing time before the 2nd plateau can be attributed to its overcharging (under-discharging), resulting from the <100% CE of TiO_2.

This cycle life of ca. 1100 is compared to CuHCF cycled in a 3-electrode cell. Fig. 3a shows the voltage profile of CuHCF cycled at 2 A g^{-1}, in 1 mol dm^{-3} $AlCl_3$, remaining stable between cycles 5000 and 25000 with a small 10% decrease in capacity. The stability of the CuHCF electrode is further illustrated in figure 3b, which gives the discharge capacity and coulombic efficiency against cycle number. Coulombic efficiency remains close to 100% throughout with capacity decreasing from an initial 35 mA h g^{-1} to 30 mA h g^{-1} after 18000 cycles at various specific currents. After 28000 cycles, capacity was approximately 26 mA h g^{-1} when cycled at 2 A g^{-1}. This is a considerably higher cycle life than reported by Liu et al for CuHCF in Al_2SO_4, likely due to the high shear mixing step employed to properly disperse, mix and homogenise active powders and binder. However, highlighted should be the importance of full cell characterisation where, despite its very high cycle life in a 3-electrode cell, the relatively low coulombic efficiency of TiO_2 results in overcharging of CuHCF and its premature degradation when employed in a full cell.

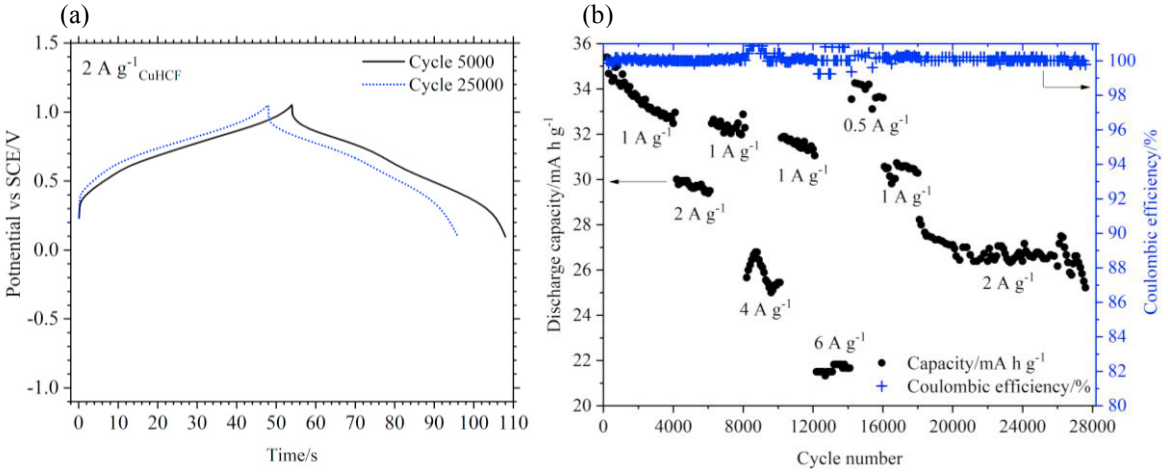

Fig. 3. Galvanostatic cyling of CuHCF in 1 mol dm^{-3} $AlCl_3$ in a 3-electrode cell. (a) Voltage profiles at 2 A g^{-1} during cycle 5000 and 25000. (b) Evolution of capacity and CE during cycling.

3.3. Degradation of CuHCF

During full cell cycling, the electrolyte gradually turned yellow, see Fig. 4 inset. The 1st plateau and primary charge storage mechanism from K^+ insertion, given by equation 1, is from the Fe^{2+}/Fe^{3+} couple [5]. It is posited that the deep oxidation of CuHCF during cell charge can lead to the presence of the 2nd plateau and Fe^{3+} in the electrolyte. The electrochemical reaction behind the 2nd plateau and the presence of Fe^{3+} in solution is still unknown. Aqueous solutions containing Fe^{3+}, such as $FeCl_3$, are known to take on a yellow-light brown colour. To investigate, UV-vis spectroscopy was performed on new electrolyte (1 mol dm^{-3} $AlCl_3$/1 mol dm^{-3} KCl) and the electrolyte used in a full cell during 1500 cycles. Fig. 4 shows the spectra of the two solutions between 250 and 650 nm. It can be seen that there is negligible absorbance shown by the new electrolyte while the used electrolyte shows significant absorbance below 280 nm with a peak centred around 337 nm, corresponding reasonably to the presence of Fe^{3+}.

$$KCuFe^{3+}(CN)_6 + xK^+ + xe^- \rightleftharpoons K_{1+x}Cu[Fe^{2+}(CN)_6]_x[Fe^{3+}(CN)_6]_{1-x} \quad (1)$$

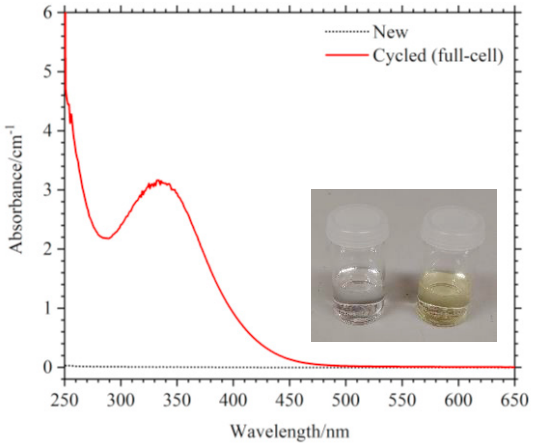

Fig. 4. UV-vis spectra of new and old electrolyte used in a full cell. Inset is a picture of the two electrolytes

4. Conclusions

Both chemical reduction and oxidation were successful in tailoring the initial SoC of CuHCF. This allowed the construction of a full cell using TiO_2 as the negative electrode. However, the CE of TiO_2 in aqueous Al^{3+} electrolyte caused premature degradation of CuHCF and a significantly reduced cycle life (from ca. 28000 to ca. 1100), highlighting the importance of full cell studies. This was due to the onset of a 2nd charge/discharge plateau which resulted in the presence of Fe^{3+} in the electrolyte, determined by UV-vis spectroscopy. Therefore, the CE of TiO_2 must be improved at low specific currents in order to produce a high rate, long cycle life aqueous Al^{3+}/K^+ battery.

Acknowledgements

Research was supported through two grants: “EPSRC Centre for Doctoral Training in Energy Storage and its Applications” EP/L016818/1 and “Horizon 2020 ALION” No 646286.

References

1. Choi, J.W. and D. Aurbach, *Promise and reality of post-lithium-ion batteries with high energy densities.* Nature Reviews Materials, 2016. **1**: p. 16013.
2. Wang, Y., et al., *Emerging non-lithium ion batteries.* Energy Storage Materials, 2016. **4**: p. 103-129.
3. Grey, C.P. and J.M. Tarascon, *Sustainability and in situ monitoring in battery development.* Nature Materials, 2016. **16**: p. 45.
4. Posada, J.O.G., et al., *Aqueous batteries as grid scale energy storage solutions.* Renewable and Sustainable Energy Reviews, 2017. **68**: p. 1174-1182.
5. Wessells, C.D., R.A. Huggins, and Y. Cui, *Copper hexacyanoferrate battery electrodes with long cycle life and high power.* Nature Communications, 2011. **2**: p. 550.
6. Park, S.I., et al., *Electrochemical Properties of NaTi2(PO4)3 Anode for Rechargeable Aqueous Sodium-Ion Batteries.* Journal of The Electrochemical Society, 2011. **158**(10): p. A1067-A1070.
7. Qu, Q.T., et al., *Electrochemical behavior of V2O5·0.6H2O nanoribbons in neutral aqueous electrolyte solution.* Electrochimica Acta, 2013. **96**: p. 8-12.
8. Pasta, M., et al., *A high-rate and long cycle life aqueous electrolyte battery for grid-scale energy storage.* Nature Communications, 2012. **3**: p. 1149.
9. Whitacre, J.F., et al., *An aqueous electrolyte, sodium ion functional, large format energy storage device for stationary applications.* Journal of Power Sources, 2012. **213**: p. 255-264.
10. Holland, A., et al., *An aluminium battery operating with an aqueous electrolyte.* Journal of Applied Electrochemistry, 2018. **48**(3): p. 243-250.